Neuron, Vol. 20, 1123–1135, June, 1998, Copyright ©1998 by Cell Press

Real Time Imaging of Calcium-Induced Localized Proteolytic Activity after Axotomy and Its Relation to Growth Cone Formation

Daniel Gitler and Micha E. Spira*
Department of Neurobiology
Institute of Life Sciences
The Hebrew University of Jerusalem
Jerusalem 91904
and the Interuniversity Institute for Marine Sciences
Eilat 88103
Israel

Summary

The emergence of a neuronal growth cone from a transected axon is a necessary step in the sequence of events that leads to successful regeneration. Yet, the molecular mechanisms underlying its formation after axotomy are unknown. In this study, we show by real time imaging of the free intracellular Ca^{2+} concentration, of proteolytic activity, and of growth cone formation that the activation of localized and transient Ca^{2+}-dependent proteolysis is a necessary step in the cascade of events that leads to growth cone formation. Inhibition of this proteolytic activity by calpeptin, a calpain inhibitor, abolishes growth cone formation. We suggest that calpain plays a central role in the reorganization of the axon's cytoskeleton during its transition from a stable differentiated structure into a dynamically extending growth cone.

Introduction

Adult neurons maintain the capacity for regrowth and structural remodeling in response to external stimuli as observed after injury (Fawcett and Keynes, 1990; Steffensen et al., 1995) or in relation to some forms of "learning"-associated processes (Lynch et al., 1990; Bailey and Kandel, 1993; Wu et al., 1995; Buchs and Muller, 1996). A neuronal compartment that plays a key role in neuronal growth during development, regeneration, and "learning"-associated processes is the growth cone (Letourneau et al., 1992). This specialized compartment, found at the tip of an extending neurite, navigates the neurite to its target while translating external cues to steering decisions (Rehder et al., 1996; Tessier-Lavigne and Goodman, 1996). It serves as the site for neurite elongation and retraction (Fawcett, 1993; Pfenninger and Friedman, 1993; Bentley and O'Connor, 1994; Lin et al., 1994; Craig et al., 1995) and, upon reaching an appropriate target, is ultimately transformed into a presynaptic terminal or a postsynaptic element (Hall and Sanes, 1993; Haydon and Zoran, 1994; Haydon and Drapeau, 1995).

The long-term extension of neurites, which is based on the transport of cytoskeletal and membrane elements from the cell body, has been studied extensively (Futerman and Banker, 1996). In contrast, little is known about the local, short-term cellular events that initiate the formation of a growth cone. Recent studies (Spira et al., 1993, 1996; Ziv and Spira, 1995, 1997; Ashery et al., 1996; Spira et al., 1998) revealed that localized and transient elevation of the free intracellular calcium concentration ($[Ca^{2+}]_i$) to 300–500 μM, caused either by axotomy or by the application of a calcium ionophore to intact cultured *Aplysia* neurons, leads to growth cone formation and irreversible neuritogenesis. These studies demonstrated that calcium-induced processes are associated with ultrastructural remodeling of the regions from which growth cones emerge (Ashery et al., 1996; Ziv and Spira, 1997) and with accelerated membrane cycling (Ashery et al., 1996). Another recent report showed that the microinjection of minute amounts of trypsin into the axon is sufficient to induce growth cone formation, resulting in irreversible neuritogenesis (Ziv and Spira, 1998).

In the present study, we examine the hypothesis that endogenous Ca^{2+}-activated neutral proteases provide the link between the elevation of $[Ca^{2+}]_i$ and the structural remodeling of the axon during its dedifferentiation into a growth cone. Calcium-activated proteolytic enzymes (calpains) are activated by $[Ca^{2+}]_i$ in the ranges of a few (μ-calpain) and of hundreds (m-calpain) of micromolars (Saido et al., 1994). Calpains display a high degree of substrate selectivity. A partial list of the cytoskeletal proteins that are cleaved by calpain includes spectrin/fodrin (Siman et al., 1984; Johnson et al., 1991), a family of proteins that serve to couple the plasma membrane to the cytoskeleton (Bennett and Gilligan, 1993; Goodman et al., 1995), as well as NCAM and N-cadherin (Covault et al., 1991), which are involved in neural cell adhesion (Doherty et al., 1995). Several members of the microtubule-associated protein family, proteins that strongly affect microtubule stability (Maccioni and Cambiazo, 1995), are also calpain substrates (Johnson et al., 1991). All of the aforementioned proteins have a role in maintaining the morphology of the adult neuron.

In the present study, we used cultured *Aplysia* neurons to examine whether calpain activation is a necessary step toward the formation of growth cones. We report that a transient and localized increase in the $[Ca^{2+}]_i$, caused by either axotomy or by the micro application of ionomycin to intact axons, induces localized proteolytic activity. The observed proteolytic activity coincides in time and space with the extension of a growth cone lamelipodium as well as with a reduction in the submembrane density of spectrin. We found that the proteolytic process, the reduction in spectrin density, and the formation of the growth cone are blocked by the calpain inhibitor calpeptin, whereas the $[Ca^{2+}]_i$ transient is not. Our observations suggest that local calcium-activated proteolysis leads to growth cone formation.

Results

Calpeptin, a Calpain Inhibitor, Abolishes Growth Cone Formation after Axotomy

Axotomy of cultured *Aplysia* neurons normally results in the rapid extension of a new growth cone from the

*To whom correspondence should be addressed.

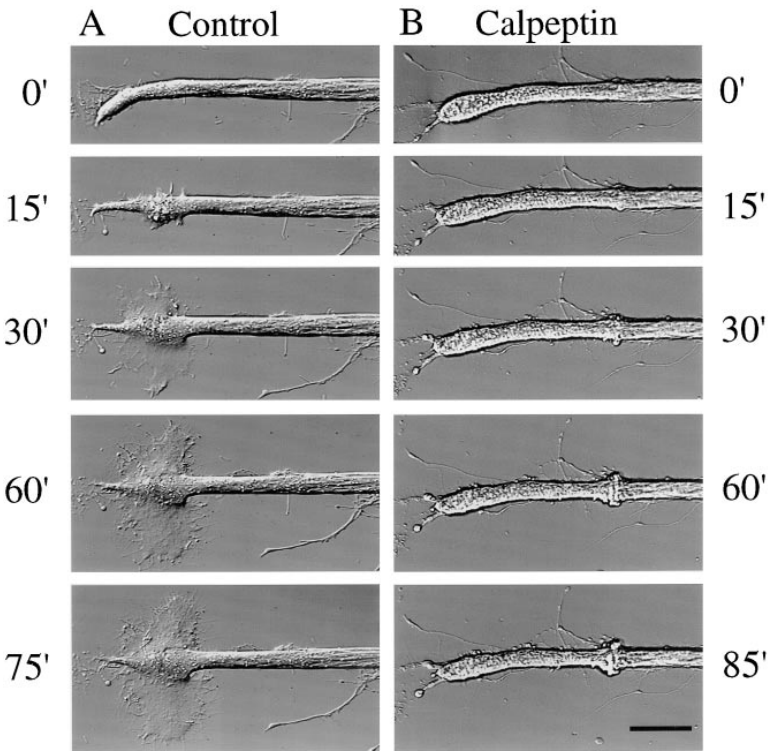

Figure 1. Calpeptin Inhibits the Formation of Growth Cones after Axotomy

Examples of *Aplysia* neurons transected in (A) ASW or (B) in ASW containing 100 μM calpeptin. The neuron that was transected in the absence of calpeptin underwent a series of morphological alterations, including flattening out of the tip and engorgement of an area 100 μm from the tip, followed by the extension of lamelipodia from that same area 15 min later. In contrast, the neuron transected in the presence of calpeptin did not manifest the aforementioned alterations and did not extend a growth cone. Time is given in minutes from axotomy. Scale bar, 50 μm.

region of the transected tip. Within minutes of axotomy, the axon's membrane reseals. Afterward, the area of the tip flattens out, while an area located 50–150 μm from the tip increases in diameter. Ten to twenty minutes from axotomy, a flat lamelipodium emerges from the enlarged area, extending later from the whole tip (Figure 1A). Subsequently, the lamelipodium breaks up into neurites, which continue extending independently. In order to investigate the possible role of calpain in growth cone formation, we transected *Aplysia* cultured neurons in artificial seawater (ASW) containing 100 μM calpeptin (Calbiochem), a membrane-permeable calpain inhibitor (Tsujinaka et al., 1988). Calpeptin did not prevent membrane resealing, as evidenced by continuous recording of the resting potential and input resistance before, during, and after axotomy (data not shown; for details of methods see Spira et al., 1993, 1996; Ziv and Spira, 1995, 1997; Ashery et al., 1996). Nevertheless, in the presence of calpeptin, axotomy was not followed by the extension of a growth cone lamelipodium (Figure 1B). In the continuous presence of the inhibitor, no growth cone was formed in 19 out of 23 transected axons. In the rest, a stunted growth cone did appear, but at a significant delay. When calpeptin was removed from the bath 30–60 min after axotomy by perfusing the bath with ASW, either no growth whatsoever occurred within the next hour (7 out of 14 experiments) or only a small growth cone appeared (7 out of 14 experiments).

Axotomy Induces a Localized Transient Elevation of the Free Intracellular Calcium Concentration and of Proteolytic Activity at the Severed Tip

The observation that the calpain inhibitor calpeptin blocks the dedifferentiation of the transected axonal tip into a growth cone suggested that calpain may be involved in the cascade of events leading to growth cone formation after axotomy. To examine this possibility, we imaged the spatiotemporal distribution of proteolytic activity and characterized its relation to the $[Ca^{2+}]_i$ gradient caused by axotomy.

To achieve this goal, we simultaneously imaged $[Ca^{2+}]_i$ using mag-fura-2 (Ziv and Spira, 1995, 1997) and proteolytic activity using the fluorogenic membrane-permeable proteolysis indicator bis(CBZ-L-Alanyl-L-Alanine amine)-Rhodamine 110 (bCAA-R110). bCAA-R110 is nonfluorescent, whereas the products of the cleavage of its amide bonds, Rhodamine 110 (R110) and its monoamides, are highly fluorescent (Leytus et al., 1983). As a result, when bCAA-R110 is cleaved by a protease, a fluorescent signal appears at the site of proteolysis.

For the experiments, neurons were injected with mag-fura-2 to reach a final intracellular concentration of 25–75 μM. Afterwards, the bathing medium was replaced by ASW containing 10 μM bCAA-R110. Images of the proteolytic activity were produced by ratioing images obtained at excitation wavelengths of 490 nm (for bCAA-R110) and 350 nm (calcium-independent mag-fura-2 signal; see Experimental Procedures), while $[Ca^{2+}]_i$ was imaged by ratioing images taken at excitation wavelengths of 380 nm and 340 nm as previously described by Ziv and Spira (1995, 1997).

As a baseline for our experiments, we monitored the proteolytic activity in intact neurons ($n = 5$; data not shown). We observed a gradual and slow increase in the fluorescent signal related to this activity. The signal reached a low steady-state level ~40–60 min after the addition of the indicator to the external solution.

We next examined the hypothesis that intracellular proteases are activated by axotomy. In these experiments, we followed the basal proteolytic activity of the

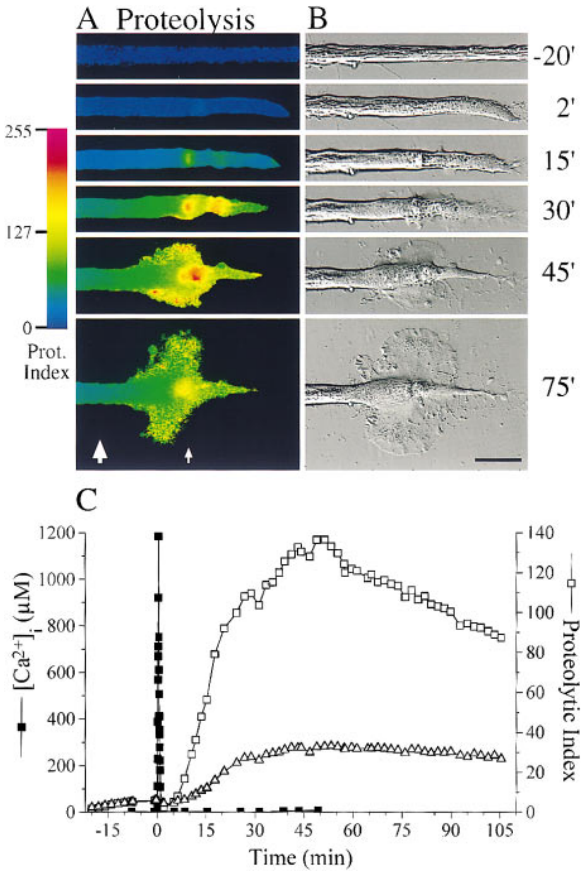

Figure 2. Axotomy Induces Proteolytic Activity

A neuron was transected while $[Ca^{2+}]_i$, (closed squares in [C]), proteolysis ([A] and open squares and triangles in [C]), and the axon's morphology (B) were monitored. Immediately upon transection, the $[Ca^{2+}]_i$ rose at the tip of the transected axon to a maximal value of 1200 μM for a duration of a few seconds (closed squares in [C]). The $[Ca^{2+}]_i$ recovered to control values in less than 5 min. Highly localized proteolytic activity developed 100 μm from the transected tip and was clearly visible within 10 min of axotomy, reaching its peak after 45 min (A and C). Growth cone extension was evident within 15 min of axotomy (B). (A) shows pseudocolor images representing the proteolytic activity within the axon immediately after bCAA-R110 was applied (−20′), just after axotomy (2′), during the increase in the proteolysis index (15′ and 30′), at the peak of the proteolytic activity (45′), and after proteolytic activity started to decrease (75′). The proteolytic activity developed in a nonhomogenous manner, with the highest value 100 μm from the transection point (small arrow). In this instance, two peaks of proteolytic activity were initially observed ([A], 15′), and these eventually merged ([A], 45′). The color bar to the left of the images encodes the extent of proteolytic activity (the proteolytic index). Time is given in minutes. (B) shows VEC-DIC images corresponding to the pseudocolor images in (A). Scale bar for (A) and (B), 50 μm. (C) shows the time course of the changes in the $[Ca^{2+}]_i$ (closed symbols) and in the proteolysis index (open symbols) in the same experiment as shown in (A) and (B). After following the basal level of proteolytic activity in the axon, the axon was transected ($t = 0$). The maximal $[Ca^{2+}]_i$ values recorded along the axon and the proteolytic index measured at a location 100 μm proximal to the transection point (small arrow in [A]) are plotted in squares. Triangles describe an additional point located a further 100 μm from the tip (large arrow in [A]).

neuron for ~20 min (Figures 2A and 2C) and then transected the axon with a sharp micropipette as previously described (Benbassat and Spira, 1993; Spira et al., 1993, 1996). As a result, the $[Ca^{2+}]_i$ level transiently increased, forming a sharp concentration gradient of >1000 μM at the tip of the axon (Figure 2C) and <100 μM at a distance of ~200 μm from the cut end. The calcium gradient declined to control values within a few minutes (Figure 2C). Axotomy was followed by a significant increase in the level of the proteolytic activity (Figures 2A and 2C). The increase was first detected ~5 min after axotomy. Initially, the proteolytic index increased in a homogeneous manner in the axoplasm, along an axonal segment 200–250 μM in length. Thereafter, discrete peaks of activity developed, in which the proteolytic index reached a maximum within 20–45 min of axotomy (Figures 2A and 2C). The proteolytic index in the rest of the tip continued rising in a slower manner. After peaking, the proteolytic activity gradually decreased. The site revealing the highest proteolytic activity always became the growth cone's center, as shown by concurrent video enhanced contrast/differential interference contrast (VEC-DIC) images of the extending growth cone (compare Figures 2A and 2B).

We noted that the focus of proteolytic activity and the site where the growth cone extended were found within an axonal segment in which the calcium concentration was maximally elevated to 200–500 μM ($n > 15$). It was therefore reasonable to assume that this range of $[Ca^{2+}]_i$ is optimal for the activation of the proteolytic activity. If this hypothesis is correct, then it is predicted that a shift of the $[Ca^{2+}]_i$ gradient along the axon would result in a corresponding shift in the site of maximal proteolytic activation and the site from which the growth cone extends.

To test this hypothesis, we imaged the proteolytic activity and the extension of the growth cone in axons transected under conditions in which $[Ca^{2+}]_i$ was raised at the axon's tip to ~200 μM (Figure 3A). This was achieved by transecting the neurons in low calcium ASW (0.5 mM instead of 11 mM) and gradually raising the calcium concentration of the external solution to 11 mM as the membrane started sealing over the cut end. In such experiments, proteolysis was manifested at the very tip of the axon and not 100–200 μm proximal to it, as occurs following transection in normal ASW (compare Figure 3B and Figure 2A). In addition, growth cone formation occurred also at the very tip (Figures 3C and 3D). These experiments ($n = 5$), and the experiments carried out in normal ASW, demonstrate a strong correlation between the $[Ca^{2+}]_i$ gradients, the proteolytic activity, and the site where growth cone formation occurs. The spatiotemporal relations described above, and the previously mentioned inhibitory action of calpeptin on growth cone formation, suggest that there exists a causal relation between the transient elevation of $[Ca^{2+}]_i$, proteolysis, and growth cone formation.

Induction of Proteolytic Activity and Growth Cone Formation by a Local and Transient Elevation of the $[Ca^{2+}]_i$ in Intact Neurons

In a recent study, Ziv and Spira (1997) showed that a focal and transient elevation of the $[Ca^{2+}]_i$ to 300–500 μM is a sufficient signal to induce growth cone formation from the axons of intact neurons. Morphologically and ultrastructurally, growth cone formation under these

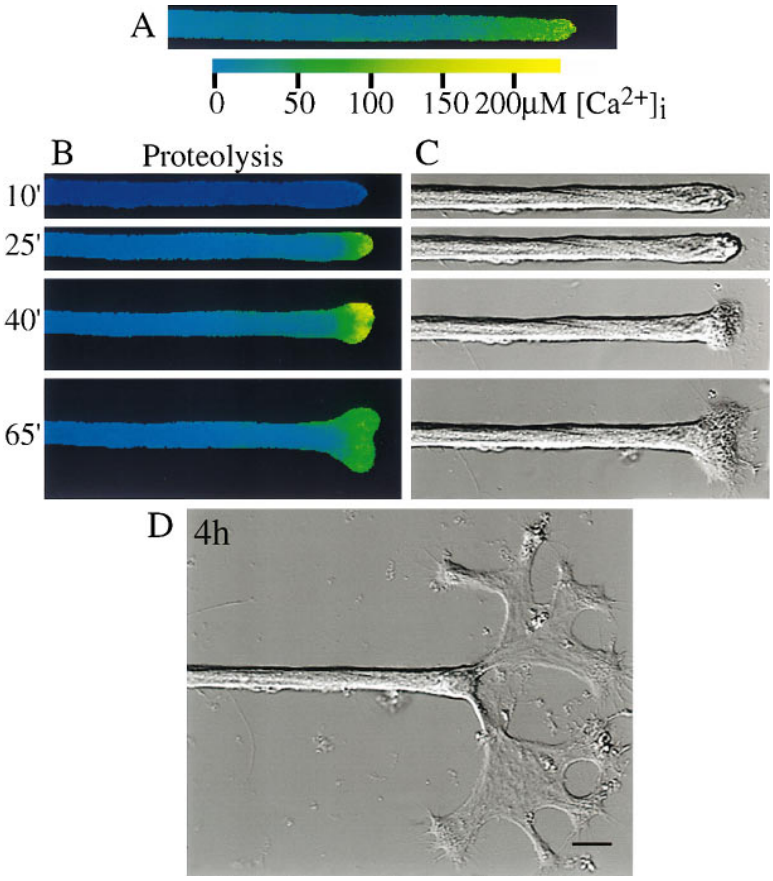

Figure 3. Proteolytic Activity and Growth Cone Formation after Axotomy in Reduced Ca^{2+} Influx Conditions

A neuron was transected in ASW containing 5% of the normal Ca^{2+} concentration while $[Ca^{2+}]_i$, proteolytic activity, and the ensuing morphological alterations were monitored. Approximately 1 min after axotomy, the bath was superfused with ASW containing increasingly higher levels of Ca^{2+} until the normal level was reached. Under these conditions, the maximal bulk $[Ca^{2+}]_i$ recorded at the tip due to Ca^{2+} influx through the cut end was reduced to 110 μM.

(A) shows a pseudocolor image of the $[Ca^{2+}]_i$ transient at its maximal level. The color bar encodes $[Ca^{2+}]_i$ levels in micromolars. (B) shows pseudocolor images of the induced proteolytic activity at various times after axotomy; (C) shows corresponding VEC-DIC images. (D) shows a VEC-DIC image of the neuron after 4 hr. Note that both the proteolytic activity and the formation of the growth cone occurred at the very tip of the transected axon (compare with Figure 2). Scale bar for (A) through (D), 50 μm.

conditions resembled the emergence of the growth cone after axotomy.

To determine whether transient elevation of $[Ca^{2+}]_i$, rather than other injury-related processes, is a sufficient signal to activate proteolysis, we focally applied ionomycin onto the axon's membrane while simultaneously monitoring $[Ca^{2+}]_i$ and proteolysis (Figure 4; n = 7). We found that proteolytic activity was induced at a restricted segment of the axon, which overlapped the part of the axon in which $[Ca^{2+}]_i$ had been elevated to 300–400 μM (Figures 4A–4D). The time course of the $[Ca^{2+}]_i$ transient and of that of the proteolytic activity was similar to that observed following axotomy (compare Figure 2C with Figure 4F). The increase in proteolytic activity was detected within 2 min of the increase in $[Ca^{2+}]_i$. Eventually, a growth cone emerged from the point where $[Ca^{2+}]_i$ and proteolysis were increased, within a time period similar to that measured in the axotomy experiments (Figure 4E). These results illustrate that a transient increase in $[Ca^{2+}]_i$ is sufficient to induce both proteolytic activity and growth cone formation.

Calpeptin Inhibits the Calcium-Induced Proteolytic Activity and Growth Cone Formation but Not the Basal Activity

In the previous sections, we have shown that proteolytic activity occurs after axotomy and that calpeptin inhibits growth cone formation. We shall now demonstrate that calpeptin inhibits the proteolytic activity.

We first characterized the effect of calpeptin on the basal proteolytic activity. We found that addition of 100 μM calpeptin to untransected neurons did not inhibit this proteolytic process (data not shown). In contrast to that, we found that in most experiments (16 out of 20 experiments), the addition of 100 μM calpeptin to the bathing solution prior to axotomy completely inhibited the proteolytic activity induced by axotomy, as well as the formation of the growth cone (Figure 5). Calpeptin did not affect the recovery of $[Ca^{2+}]_i$ to control levels once the membrane resealed (Figure 5C), suggesting that calpeptin does not alter the Ca^{2+} handling power of the neuron. In those experiments where a stunted growth cone did extend in the presence of calpeptin, weak proteolytic activity was observed at the growth cone's base (4 out of 20; data not shown). Removal of calpeptin from the dish after axotomy always resulted in an immediate increase in the rate of proteolysis (n = 14; data not shown). In half of these experiments, growth cones did not extend within an hour, a period of time within which growth cones invariably emerge in control conditions. In the rest of these experiments, a small growth cone did extend from the location where proteolytic activity was evident. A possible explanation for these results is that the concerted activation of additional enzymatic processes is needed to enable the formation of the growth cone (see Discussion).

Consistent with the results described above, calpeptin inhibited both the proteolytic activity induced by the focal application of ionomycin and the formation of a growth cone (n = 4; Figure 6). In the experiment described in Figure 6, ionomycin was applied to the same axon at two locations, before and after the addition of

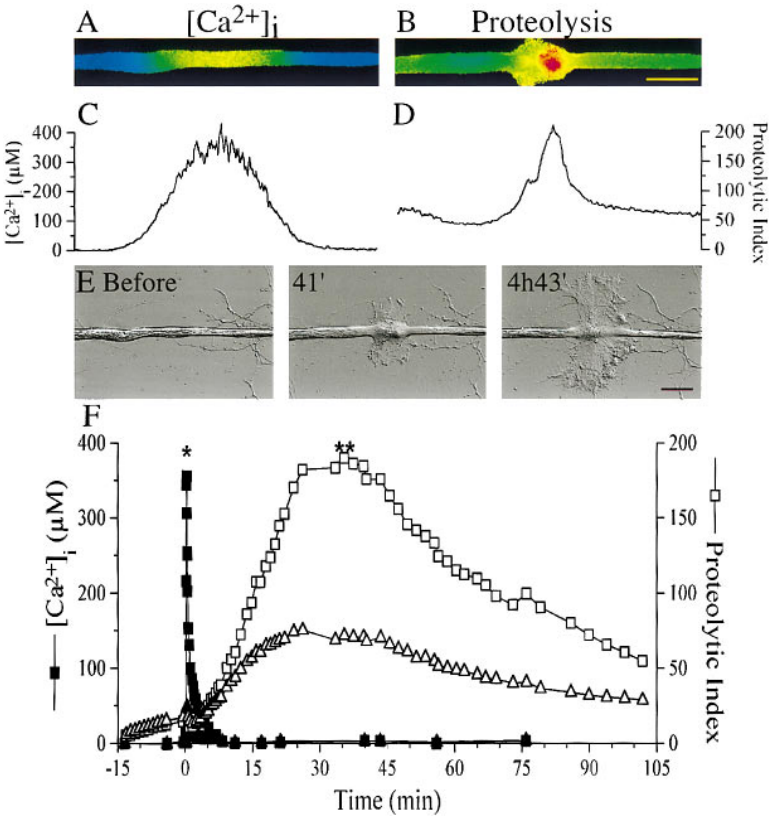

Figure 4. Raising $[Ca^{2+}]_i$ by the Focal Application of Ionomycin Induces Both Colocalized Proteolysis and Growth Cone Formation

500 μM ionomycin (in ASW) was focally and briefly applied to an arbitrary point along the axon by microejection. As a result, $[Ca^{2+}]_i$ was raised transiently to 300–400 μM at that location (A and C), and thereafter highly localized proteolytic activity developed at that point (B and D), concurrent with the extension of an ectopic growth cone from the same location (E). (A) and (B) show pseudocolor images of the maximal $[Ca^{2+}]_i$ (A) and maximal proteolytic activity (B) levels attained after the application of ionomycin. (C) and (D) show corresponding spatial profiles of $[Ca^{2+}]_i$ and proteolysis. Scale bar for (A) through (D), 50 μm. (E) shows VEC-DIC images of the same area shown in (A) and (B), taken during growth cone emergence. Time in (E) is given from ionomycin application. Scale bar for (E), 50 μm. (F) shows the time course of the $[Ca^{2+}]_i$ transient (closed symbols) and of the proteolytic activity (open symbols). The values depicted by squares in both plots were obtained at the location where the proteolytic activity was highest as seen in (B). Triangles denote an area located 120 μm distal to that location (to the right). The asterisk (*) denotes the time point when (A) was obtained, whereas the double asterisk (**) marks the time when (B) was acquired. Time is given in minutes, referring to ionomycin application as time zero. Note the similarity between the time courses presented here and those produced after axotomy (Figure 2).

calpeptin to the external medium. The ionomycin applications were executed in such a way that $[Ca^{2+}]_i$ was raised to approximately the same level and for the same length of time in both instances. The application of ionomycin in the absence of calpeptin was followed by the local activation of proteases and by growth cone extension (left images in Figures 6B–6E). In contrast, the same treatment in the presence of calpeptin failed to induce either a local proteolytic response or growth cone formation (right images in Figures 6B–6E).

These results imply that the basal proteolytic process and the calcium-induced one are unrelated, as they are inhibited differently by the same inhibitor. Only the calpeptin-sensitive protease plays a role in the calcium-induced dedifferentiation of an axon into a growth cone.

Reduction in Spectrin Density Spatially Correlates with Increased Levels of Proteolytic Activity and with the Formation of the Growth Cone

Aunis and Bader (1988) and Perrin et al. (1992) suggested that removal of spectrin makes the inner surface of secretory cells accessible for fusion with intracellular membranes. As spectrin is a substrate of calpain, and since the growth process requires the insertion of intracellular membranes into the neurolema, we next studied the relations between calcium-induced proteolysis, the distribution of axonal spectrin, and the formation of the growth cone. For this purpose, we transected the neurons, measured both the $[Ca^{2+}]_i$ transient and the ensuing proteolytic activity, and then immunolabeled the neurons with anti-spectrin antibodies (n = 11; Figure 7). Confocal microscopic images of control neurons revealed that spectrin is abundant at the submembrane domain and less so in the inner axonal space (Figure 7A). We found that axotomy greatly reduces the density of submembrane spectrin in regions where the $[Ca^{2+}]_i$ was elevated and in which proteolytic activity was induced. Figure 7D depicts spectrin staining in an axon fixed 18 min after axotomy. In this example, spectrin was removed from the focus of proteolytic activity (Figure 7C) and from the submembrane domain at the tip, without affecting appreciably its inner axonal density. Note that this neuron was in the initial stages of growth cone formation, as evidenced by the small area of the emerging lamelipodium (arrowhead in Figure 7B). In an axon fixed 25 min after axotomy (Figures 7E–7G), the spectrin staining density was reduced in the whole tip (Figure 7G). This neuron extended an appreciable lamelipodium before being fixed (Figure 7E). In both instances, an abrupt drop in spectrin density was observed in the same region where the proteolytic activity was most intense (compare Figures 7D and 7G with 7C and 7F). This region overlaps with the site from which the growth cone invariably emerges (Figures 7B and 7E). We found that when proteolysis was inhibited by calpeptin, spectrin density did not decrease. Under these conditions, spectrin was found to surround the whole of the axon, up to the very tip (n = 8; Figure 7H). These results are consistent with the possibility that Ca^{2+}-dependent proteolytic processes remove the spectrin-based membrane skeleton and thereby facilitate the insertion of intracellular membranes into the neurolema.

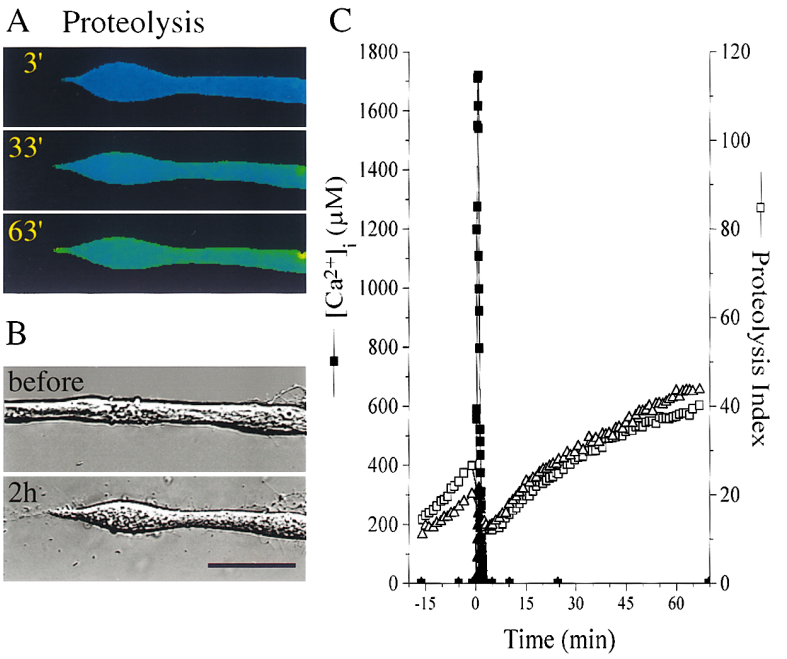

Figure 5. Calpeptin Abolishes Both the Proteolytic Activity and the Formation of the Growth Cone Caused by Axotomy

The axotomy experiment described in Figure 2 was repeated in the presence of 100 μM calpeptin.

(A) shows representative pseudocolor images of the proteolytic activity within the transected axon at various time points. Time is given in minutes from axotomy. (B) shows VEC-DIC images illustrating that the formation of the growth cone was completely abolished by the inclusion of calpeptin in the bath medium. Scale bar for (A) and (B), 50 μm. (C) shows the time course of the $[Ca^{2+}]_i$ transient (closed symbols) and of the proteolytic activity (open symbols) occurring after axotomy (t = 0). Even though $[Ca^{2+}]_i$ rose to ~1700 μM, no additional proteolytic activity was initiated by axotomy. There was no evident change in the rate of proteolysis before and after axotomy, and the proteolytic index continued rising slowly throughout the duration of the experiment. The only effect of axotomy was an abrupt drop in fluorescence that occurred during axotomy. The values plotted with squares were obtained from an area located near the axon's tip, whereas triangles designate an axonal area found 80 μm proximal to the tip.

Discussion

This is the first report to directly identify the involvement of calcium-induced intracellular proteolysis in the process of growth cone formation after axotomy. We found that a transient increase in the $[Ca^{2+}]_i$, caused by axotomy or by transient elevation of $[Ca^{2+}]_i$ in axons of intact neurons, leads to localized proteolytic activity, to a reduction in the submembrane density of spectrin, and to growth cone formation. Inhibition of the proteolytic

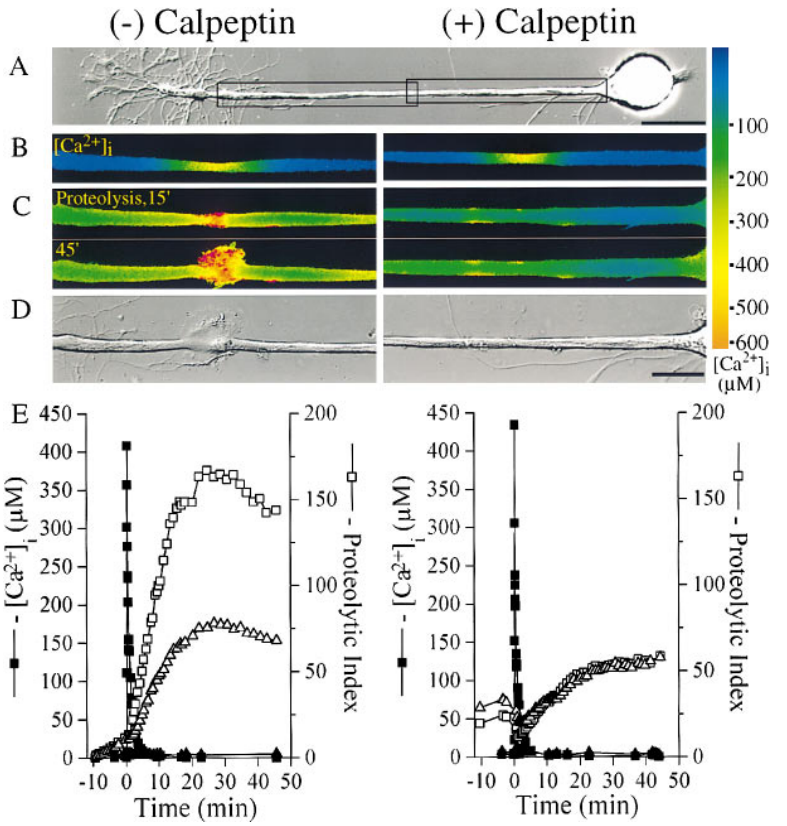

Figure 6. Calpeptin Inhibits Proteolysis and Growth Cone Formation Elicited by the Application of Ionomycin

Ionomycin was applied to the same neuron twice, at first in the absence of calpeptin (left images) and then 10 min after the application of 75 μM calpeptin to the bathing solution (right images). The application of ionomycin was performed so that the change in $[Ca^{2+}]_i$ was comparable in both instances.

(A) shows a VEC-DIC image of the neuron taken before the ionomycin applications. Rectangles mark the areas shown in the higher magnification images (B–D). (B) shows pseudocolor images of the $[Ca^{2+}]_i$ acquired during its maximal increase. A $[Ca^{2+}]_i$ calibration scale bar is supplied to the right. (C) shows pseudocolor images of the proteolytic activity acquired 15 and 45 min after ionomycin application. (D) shows VEC-DIC images taken 45 min after ionomycin application. Notice that a growth cone extended in the left image (−calpeptin), whereas no growth whatsoever is evident in the right image (+calpeptin). Scale bar for (A), 100 μm; for (B) through (D), 50 μm. (E) shows concurrent monitoring of $[Ca^{2+}]_i$ (closed symbols) and proteolysis (open symbols) at the application point (squares) and at a distance of 100 μm (triangles) in the absence (left) and presence (right) of calpeptin. As can be seen, calpeptin inhibited the inducible proteolytic activity, and as a result no spatial gradient is evident.

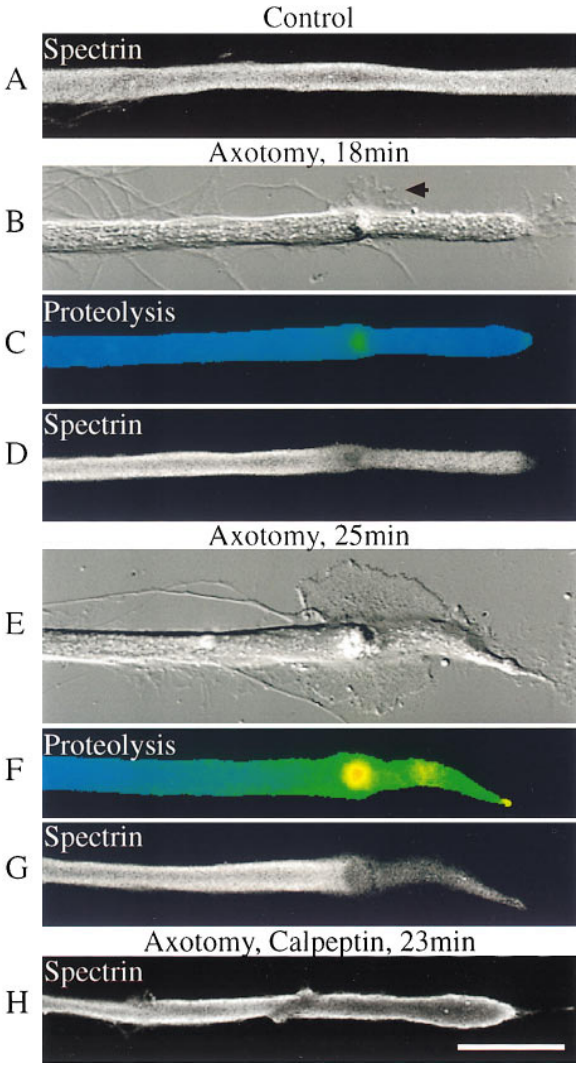

Figure 7. Axotomy Reduces Spectrin Density at the Transected End in a Calpeptin-Sensitive Manner

Proteolysis was monitored in transected neurons, which were subsequently fixed and fluorescently immunolabeled for spectrin. (A) shows spectrin immunolabeling of an untransected axon. Notice that spectrin staining is brighter in the submembrane domain of the axon. (B) shows a VEC-DIC image of a transected axon, taken 18 min after axotomy and just prior to fixation. The growth cone is just beginning to emerge, and appears as a small lamelipodium (arrowhead). (C) shows a pseudocolor image of the proteolytic activity as observed just prior to fixation in the same axon. (D) shows spectrin immunolabeling of the axon. Spectrin density was reduced in the axon in two ways. First, spectrin was removed from the submembrane domain at the region of the tip, without changing much of the intraaxonal density. In contrast, spectrin density was decreased in both the core and the cortex of the axon, in the region where proteolytic activity is evident in (C). (E) shows a VEC-DIC image of a transected axon, at a more advanced stage of the emergence of a growth cone. The image was taken 25 min after axotomy and just prior to fixation. A full-fledged lamelipodium is evident. (F) shows a pseudocolor image of the proteolytic activity in the same axon. (G) shows spectrin immunolabeling of the axon seen in (E) and (F). In this instance, spectrin density is reduced from the point where the maximal proteolytic activity was recorded, up to the tip. (H) shows spectrin immunolabeling of an axon transected in the presence of 100 μM calpeptin. The neuron was fixed 23 min after axotomy. Note that spectrin was not removed from the submembrane domain, so that it ensheaths the whole axon, up to the tip. Scale bar for (A) through (H), 50 μm.

activity by calpeptin inhibits both the reduction in the density of spectrin and the formation of the growth cone, without preventing the removal of Ca^{2+}. We thus suggest that calcium-induced localized proteolysis is a necessary step in the cascade of events leading to growth cone formation following axotomy.

Calcium-induced proteolytic activity was detected in the axoplasm as early as 2–5 min after the induction of a localized increase in $[Ca^{2+}]_i$, caused either by the application of ionomycin or by axotomy (Figures 2 and 4). We presume that earlier stages of the calcium-induced proteolysis were not detected by us, as the initial fluorescent signal produced by the proteolytic product R110 must have been too faint. The bulk axonal proteolytic activity reached a peak within 20–45 min and thereafter decelerated so that the fluorescent signal reporting it decreased to control levels within an additional hour. Similar kinetics have been reported for the initial detection of calpain activity in human platelets. The cleavage of talin, of actin-binding protein, and of phospholipase C 3β is initially detectable within ~5 min of the incubation of platelets in a solution including 1 μM of the calcium ionophore A23187. Proteolysis proceeds for >20 min, as seen in SDS-PAGE gels and Western blots (Banno et al., 1995).

The maximal level of proteolytic activity was observed in a region in which the calcium concentration had previously reached a level of 300–500 μM. Segments found proximal ($[Ca^{2+}]_i < 200$ μM) and distal ($[Ca^{2+}]_i > 600$ μM) to this region revealed lower levels of proteolysis. The growth cone's lamelipodium consistently emerged from this region.

Characterization and Mode of Action of the Calcium-Induced Intracellular Protease

A central question concerning our observations is the identity of the protease responsible for the activity reported by us and its mode of action. The properties of the protease activated by axotomy or transient elevation of $[Ca^{2+}]_i$, and its relation to growth cone formation, suggest that it is calpain. This is based on the following: calpeptin, a membrane-permeable calpain inhibitor (Tsujinaka et al., 1988), inhibits the proteolytic activity induced by either axotomy or by a transient elevation of the free intracellular calcium concentration but does not inhibit the basal proteolytic activity recorded in intact neurons. In addition, there exists a strong spatial correlation between the $[Ca^{2+}]_i$ transient and the observed proteolytic activity. Finally, the submembrane density of spectrin, a well-known substrate of calpain, is reduced during the formation of the growth cone.

Consistent with this point of view is the characteristic dependence of calpain on calcium for its activation and the subsequent lower dependence of calpain on calcium after autoproteolysis (Saido et al., 1994; Kawasaki and Kawashima, 1996). Based on the temporal relations between the $[Ca^{2+}]_i$ transient and the activation of the proteolytic activity, we assume that calpain is autoproteolyzed during the initial surge of $[Ca^{2+}]_i$ and then remains

active at lower $[Ca^{2+}]_i$ levels. Calpain is gradually further autoproteolyzed and so becomes inactive (Nishimura and Goll, 1991; Raser et al., 1995). In addition, it is dispersed with the membrane vesicles to which it is bound (see below).

Various types of calpain have been identified, including m-calpain, which is activated by concentrations of calcium ions in the range of hundreds of micromolars, and μ-calpain, which is activated at the low micromolar level (Saido et al., 1994; Kawasaki and Kawashima, 1996). Since at least 200 μM $[Ca^{2+}]_i$ is needed to initiate growth cone formation when ionomycin is applied to the axon (Ziv and Spira, 1997), we tentatively attribute the observed proteolytic activity to m-calpain.

We showed that besides the calcium-induced proteolytic activity, the neuron also exhibits continuous low level basal activity, which is not affected by calpeptin. We do not know the nature of this activity or the identity of its effector.

The Spatiotemporal Distribution of the Proteolytic Activity and Its Relation to Growth Cone Extension

Inactive calpain is considered to be a soluble enzyme homogeneously distributed throughout the cell's interior. Its activation is thought to be associated with its translocation to membranes (Goll et al., 1992; Kumamoto et al., 1992; Kawasaki and Kawashima, 1996). Since the proteolysis substrate, bCAA-R110, and its product, R110, are both of small molecular weight, it would be expected that following the induction of proteolytic activity, the fluorescent product would be distributed along a long axonal segment, encompassing at least the area in which high $[Ca^{2+}]_i$ levels were recorded. Our results show, however, that initially only a narrow profile of proteolytic activity is formed (see Figures 2 and 4). It is not probable that this is due to the accumulation of either bCAA-R110 or R110 at that location, since both substances are membrane permeable. A more plausible explanation would be that the processing protease accumulates at that site. This would be possible if activated calpain became associated with an intracellular structure located at the site where the growth cone emerges.

Previous studies revealed accumulation of retrieved axolemal membrane at the axon's center, at the location from which the growth cone eventually emerges (Ashery et al., 1996; Ziv and Spira, 1997). Since calpain has been reported to bind to membranes and vesicles (Ariyoshi et al., 1992; Sato et al., 1995; Melloni et al., 1996), it is possible that after its activation by calcium, a fraction of the active calpain associates with the inner face of the axolema, while another fraction associates with the retrieved axolemal membrane. The very large density of retrieved membrane at this location may account for the focused fluorescent signal of the proteolytic product recorded from this location.

The Relation between Growth Cone Formation and Calpain Activation

Based on the results described here, as well as those described in earlier studies (Spira et al., 1993, 1996, 1998; Ashery et al., 1996; Ziv and Spira, 1997, 1998), we tentatively suggest the following cascade of events to underlie the process of growth cone formation after axotomy of cultured *Aplysia* neurons. The culturing procedure primes the neurons for growth by upregulating the expression of proteins that are essential for growth processes (Ambron et al., 1996). A transient localized increase in the free intracellular calcium concentration, from a resting level of ~0.1 μM to 200–500 μm, triggers the activation of cytoplasmic calpains. The calcium-activated calpains undergo autoproteolysis and are translocated to the plasma membrane, subcellular organelles, and endocytotic vesicles. The axolema- and vesicle-bound calpains induce extensive remodeling of the membrane skeleton and cytoskeleton. These alterations underlie two main processes essential for the initiation of growth cone extension: the local dissociation of cytoskeletal elements produces a region in which transported and endocytosed vesicles accumulate. These vesicles form a membrane store, available for the extension of the growth cone. The second essential process is the exposure of the inner face of the plasma membrane by the removal of the spectrin-based membrane skeleton. The exposed membrane is made accessible for the fusion of intracellular vesicles (Aunis and Bader, 1988; Perrin et al., 1992). Subsequently, microtubules extend perpendicularly to the membrane (Ziv and Spira, 1997) from newly exposed nucleation sites (Yu et al., 1994; Baas, 1997). The microtubules direct membrane vesicles to the plasma membrane through rapid axonal transport mechanisms (Martenson et al., 1993), thus supplying locally accumulated building materials to the nascent growth cone. Eventually, long term mechanisms supply the needs of the extending growth cone.

We showed that removal of calpeptin within 20–30 min of axotomy reversed at least some of its inhibiting effects. The ensuing proteolytic activity nevertheless failed in half of the cases to produce growth cones (7 out of 14 experiments), whereas such growth as did occur was limited. It is probable that growth cone formation necessitates the concerted activation of various enzymatic processes. Therefore, it is conceivable that deferring proteolytic activity, by its temporary inhibition, interferes with the converging activity of several enzymatic processes that underlie growth cone formation. One group of enzymes that are possible candidates for such a role are the protein kinases, since they are known to modulate the extension of neurites (Maness, 1992; Goldberg and Wu, 1996).

Calcium, Cytotoxicity, Neuronal Remodeling, and Regrowth

Calcium is known to be toxic to cells, as happens during excitotoxicity (Rothman and Olney, 1995). Recent research has found a connection between excitotoxicity and calpain activation (Brorson et al., 1994; Saido et al., 1994; Bednarski et al., 1995). It was shown that neuronal survival after trauma such as hypoxia and ischemia can be enhanced by the inhibition of calpains (Wang and Yuen, 1994). The results and the hypothesis we presented above require the elevation of $[Ca^{2+}]_i$ to levels well within what is currently believed to be toxic to the

cell (see also Ziv and Spira, 1997). Indeed, when in experiments similar to those reported here $[Ca^{2+}]_i$ was elevated for longer periods of time or to higher calcium concentrations, the neurons revealed degenerative processes in the form of blebbing or beading. It seems to us that growth cone formation can be induced only by increases in $[Ca^{2+}]_i$ that are narrowly confined in terms of concentration and duration of exposure. Lower concentrations do not trigger the formation of growth cones (Ziv and Spira, 1997), while long exposures (several minutes) of high concentrations of $[Ca^{2+}]_i$ induce degeneration.

We propose that a $[Ca^{2+}]_i$ transient similar to that reported here may occur in submembrane domains in relation to the induction of growth cone formation under physiological conditions. It is of interest to note that $[Ca^{2+}]_i$ levels in the range of hundreds of micromolars have been previously described to occur in submembrane domains of presynaptic elements (Llinas et al., 1992). The findings presented here are consistent with earlier studies that suggest a role for calpain activity in morphological remodeling of neurons in relation to "learning"-related processes (Lynch and Baudry, 1984; Lynch et al., 1990). In these studies, it was suggested that calpain activity participates in processes such as long-term potentiation (LTP) by perpetuating morphological changes in preexisting structures. This suggestion is based on the detection of calpain-generated spectrin fragments in NMDA-treated hippocampal slices (Seubert et al., 1988; del Cerro et al., 1994), as well as in slices that have been stimulated at the theta rhythm, a rhythm that is known to stimulate the production of LTP (Vanderklish et al., 1995). Translational suppression of calpain expression in such slices reduced the formation of spectrin fragments (Bednarski et al., 1995). In addition, inhibition of calpain altered the process of LTP generation (del Cerro et al., 1990).

A recent study has linked calpain activation with remodeling of dendrites after sublethal excitotoxic injury in vitro, as assessed by immunolabeling of both MAP2- and calpain-generated spectrin fragments (Faddis et al., 1997). This study showed that calpain activation is associated not with the formation of injury-induced varicosities but rather with their dissolution, thus supporting our suggestion that calpain activation has a role in recovery from injury. In this study, as in ours, calpain was activated for a time period of >1 hr, long after the injurious insult had been removed.

We propose that in neurons primed for growth, a transient increase in $[Ca^{2+}]_i$ to the submillimolar range may manipulate subtly and locally the neuron's cytoskeleton, ultimately inducing controlled growth cone formation.

Experimental Procedures

Cell Cultures

Neurons B1 and B2 from buccal ganglia of *Aplysia californica* were isolated and maintained in culture as previously described (Schacher and Proshansky, 1983; Benbassat and Spira, 1993; Spira et al., 1996). Briefly, buccal ganglia were isolated and incubated for 1.5–2.5 hr in 1% protease (type IX, Sigma) at 35°C. The ganglia were then desheathed, and the cell bodies of the buccal neurons with their long axons were pulled out with sharp micropipettes and placed on poly-L-lysine–coated (Sigma) glass bottom culture dishes. The culture medium consisted of equal parts of filtered hemolymph from *Aplysia faciata* collected along the Mediterranean coast and L-15 (Gibco-BRL) supplemented for marine species. All experiments were performed 8–36 hr from plating, after replacing the culture medium with ASW (NaCl 460 mM, KCl 10 mM, $CaCl_2$ 10 mM, $MgCl_2$ 55 mM, and HEPES [N-(2-hydroxyethyl)piperazine-N′-2-ethanesulfonic acid, Sigma] 10 mM, adjusted to pH 7.6).

Axotomy

Axonal transection was performed by applying pressure on the axon with the thin shaft of a micropipette under visual control, as has been previously described (Benbassat and Spira, 1993, 1994; Spira et al., 1993, 1996; Ziv and Spira, 1993, 1995).

Elevation of the Free Intracellular Ca^{2+} Concentration by the Application of Ionomycin

A local and transient elevation of the free intracellular calcium concentration ($[Ca^{2+}]_i$) was achieved by locally applying ionomycin from a micropipette onto the axonal membrane as previously described (Ziv and Spira, 1997). Briefly, ionomycin (calcium salt, Sigma) from a stock solution of 10 mM in dimethyl sulfoxide (DMSO) was diluted with ASW to a final concentration of 0.5 mM and focally applied by pressure ejecting the solution onto the axonal membrane with a micropipette. The alterations in the $[Ca^{2+}]_i$ were monitored online by mag-fura-2 imaging as described below. Ejection of the carrier solution did not elevate the $[Ca^{2+}]_i$, nor did it induce morphological changes.

Video Microscopy

The system used for DIC video microscopy consisted of a Zeiss Axiovert microscope equipped with DIC optics, a long working distance condenser set for Koehler illumination, and a 100 W halogen light source. The objectives used were either a Zeiss 20× 0.50 NA Plan-Neofluar objective or a Zeiss 40× 0.75 NA Plan-Neofluar objective. Images were collected by grabbing and averaging 32 video frames produced by a Vidicon video camera (Hamamatsu). Grabbing was done online with a frame grabber (Imaging Technologies). After the experiment, the resulting images were enhanced by subtracting the image of an empty area of the culture dish and then by adjusting the contrast by histogram stretching. The final images were prepared using commercially available software (Adobe Photoshop).

Mag-fura-2 Ca^{2+} Imaging

Mag-fura-2 loading, imaging, and calibration were done as previously described (Ziv and Spira, 1995, 1997). Briefly, the neurons' cell bodies were impaled with a microelectrode containing 2 M KCl and 10 mM mag-fura-2 (Molecular Probes), and the indicator was loaded by pressure injection to a final concentration of 25–75 μM. Imaging was performed after the dye had equilibrated throughout the main axon (~30 min). Fluorescence images of the neurons loaded with mag-fura-2 were taken by real-time averaging of 16 video frames at 340 ± 5 nm and 380 ± 5 nm excitation wavelengths. Background images, obtained from regions adjacent to the neuron to be tested, were subtracted from the averaged images obtained at both wavelengths. Ratio images of the fluorescent intensities were obtained by dividing each pixel in the 340 nm fluorescence image by the corresponding pixel in the 380 nm fluorescence image. The ratio values were converted to free intracellular Ca^{2+} concentrations by means of calibration curves prepared as previously described (Ziv and Spira, 1995, 1997).

The fluorescent microscope system consisted of a Zeiss Axiovert microscope equipped with a 75 W Xenon arc lamp; a Zeiss 40× 0.75 NA Plan-Neofluar objective; 340 ± 5 nm and 380 ± 5 nm band-pass excitation filters set in a computer-controlled, 10 position filter changer (Lambda); a dichroic mirror with a cutoff threshold of 500 nm; and a 545 ± 25 nm band-pass emission filter. The images were collected with a CCD video camera (Hamamatsu) equipped with an image intensifier, digitized with a PC hosted frame grabber (Imaging Technologies), stored as computer files, and processed using a software package written in our laboratory.

Proteolytic Activity Imaging

Neurons that were previously loaded with mag-fura-2 were continuously incubated in ASW containing 10 μM bis(CBZ-Alanyl-Alanine amine)-Rhodamine 110 (bCAA-R110, Molecular Probes) (Leytus et al., 1983) and were imaged to determine the level of proteolytic activity. Ratio imaging was performed as described for mag-fura-2 except that the excitation wavelengths used were 490 ± 6 nm, which excites Rhodamine 110 (R110), and 350 ± 5 nm, which excites mag-fura-2.

The formation of a growth cone, after both axotomy and the application of ionomycin, is associated with local changes in the neurons' morphology. Under these conditions, the obtained fluorescent images report changes in the quantity of the fluorophore, attributable to changes both in concentration and in volume. To correct for the volume changes, images obtained while exciting at 490 nm, which represent the release of fluorescent proteolysis products (R110 and its monoamide), were divided by images obtained at 350 nm, which represent the local cell dimensions, as reported by mag-fura-2 fluorescence. Since 348 nm is mag-fura-2's isosbestic point, as determined by us in calibration solutions (KCl 250 mM, EGTA 7 mM, $MgCl_2$ 2 mM, $CaCl_2$ 0–100 mM, and HEPES 20 mM [pH 7.4]; data not shown), images taken at 350 nm are hardly affected by changes in $[Ca^{2+}]_i$. It is important to note that the level of interference between mag-fura-2 and R110 is small, because they are excitable at mutually exclusive ranges of the spectrum. To ascertain that the interference is small in practice, cells loaded with mag-fura-2 were imaged with R110 optics and vice versa. We found that R110 does not noticeably contribute to mag-fura-2 images, while mag-fura-2, at the concentrations used, offsets the observed fluorescence of R110 by ~2% of the peak values. This means that most "R110" fluorescence observed at the beginning of the experiment is contributed by mag-fura-2, but as soon as R110 is produced, this distortion becomes insignificant. The axons' autofluorescence at both wavelengths is negligible.

The decrease in mag-fura-2 fluorescence, due to its leakage out of the neuron during the experiment, is in the range of 10%. This means that the total error, introduced by ratioing against mag-fura-2 images obtained at an excitation wavelength of 350 nm, is 11% at most. The distortion caused by mag-fura-2 leakage was corrected by dividing each ratio image by the fraction of mag-fura-2 left in the neuron at that time. In order to calculate the fraction of mag-fura-2 left in the neuron, a reference area was defined, in which no volume changes were observed (as determined by VEC-DIC) and in which no $[Ca^{2+}]_i$ changes were evident throughout the experiment. The mag-fura-2 fraction was then calculated by dividing the fluorescence intensity value in the reference area in each image by the initial value of the same area at the beginning of the experiment.

The image-processing manipulations introduced above produce images corrected for spatial and temporal distortions in a reproducible manner. The resulting units of activity were termed "proteolysis index." Proteolysis index values are comparable within an image, throughout the duration of an experiment. However, values cannot be compared between experiments.

Determination of the Spatial and Temporal Resolution of the Proteolytic Processes

The fluorescent signal of the cleaved product of bCAA-R110 reliably provides the rate and location of the calcium-induced proteolytic activity. This conclusion is based on a series of experiments in which we characterized the permeability and the diffusion coefficient of the fluorescent product R110 and the proteolysis substrate bCAA-R110.

We found both R110 (Molecular Probes) and bCAA-R110 to be membrane permeable. The permeability of bCAA-R110 is confirmed by the detection of its cleavage product, R110, inside an axon after inducing proteolytic activity by the application of ionomycin (Figure 4) or by the detection of intracellular proteolytic activity when bCAA-R110 was added to the bath medium after the resealing of the membrane (data not shown).

The permeability of R110 was tested by examining the fluorescence that was retained in an axon after incubating a neuron in ASW containing 1 μM R110 and perfusing the bath rapidly with R110-free ASW (Figure 8A). This protocol also enabled us to measure the rate of efflux of R110. We found that R110 leaks through the plasma membrane with a time constant of 211 ± 66 s (n = 9). In order to make sure that R110 is not retained in the transected tip as a result of an axotomy-dependent process, we performed the above described measurement on newly transected neurons (data not shown). We found transection of the neuron prior to the removal of R110 not to have any effect on the measured efflux rate.

We also determined the diffusion coefficient of R110 inside an axon by the method of Gabso et al. (1997) and found it to diffuse

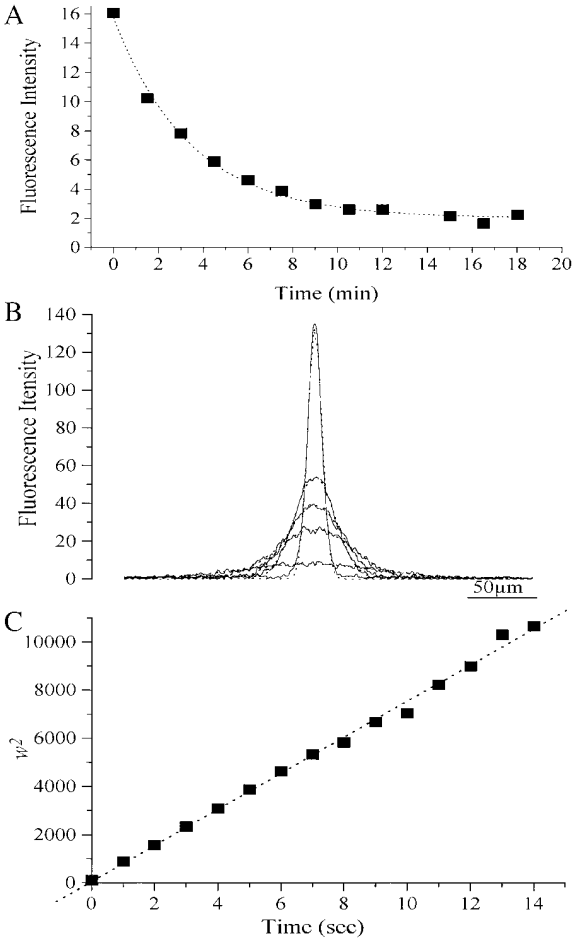

Figure 8. Determination of Dispersion-Related Parameters of R110

(A) shows the time constant of the leakage of R110 from an intact axon. An untransected neuron was bathed in ASW containing 1 μM R110 for 25 min. The bath solution was then exchanged with R110-free ASW, and the efflux rate of R110 was determined by measuring the decrease in fluorescence intensity at an arbitrary point along the axon. The fluorescence intensity of the axon decayed in a purely exponential manner. In the example shown here, the time constant was determined to be 3 min and 27 s. Time is given in minutes from the acquisition of the first image. (B) and (C) show the determination of the intracellular diffusion coefficient of R110 (DR110). In (B), 100 μM R110 (in 2 M KCl) was injected for a duration of 50 ms into a cylindrical axon. The resulting diffusion profiles were collected (solid lines) and were fitted to Gaussian plots (dashed lines). For clarity purposes, only the profiles for 0, 1, 2, 4, and 14 s after injection are shown. In (C), the square of the width parameter of the Gaussians was plotted as a function of the time from injection and DR110 was extracted from the slope of the fitted line (see the Experimental Procedures). In the example presented here, DR110 was found to be 93.66 $\mu m^2/s$.

rapidly with a diffusion coefficient of 68.8 ± 15 $\mu m^2/s$ (n = 8) (Figures 8B–8C).

Briefly, the axon of an untransected neuron was impaled with a sharp microelectrode containing 100 μM R110 in a 2 M KCl solution. R110 was then pressure injected into the axon for a duration of 50 ms. The dispersal of R110 was followed by imaging the axon at fixed time intervals at an excitation wavelength of 490 ± 6 nm. An image of the fluorescence observed prior to the injection of the dye was subtracted in order to set the baseline to zero. The diffusion coefficient was calculated by fitting a model of one-dimensional diffusion to the experimental data. This method is applicable to our preparation because the axons maintain a long cylindrical morphology in culture, and since the radial equilibration of R110 is fast. This model can be described by the well-known function:

$$y(x,t) = \frac{A \exp(-x^2/(4Dt))}{\sqrt{4\pi Dt}}$$

where t is the time from injection, x is the distance from the point of injection, y(x,t) is the fluorescent signal of the dye at location x and time t, A is a proportion constant relating to the quantity of the dye injected, its fluorescence parameters, the specific radius of the axon, and the optical setup, and D is the diffusion coefficient of the dye.

At any given time t, the dispersion of the dye is described by the Gaussian $y_t(x)$. We can mark $w = \sqrt{8Dt}$, where w is the width parameter of the Gaussian, and then the above equation is reduced to:

$$y_t(x) = \frac{A \exp(-2x^2/w^2)}{w\sqrt{\pi/2}}$$

Hence, by fitting Gaussians to plots of the observed fluorescent intensity along an injected axon taken at fixed time intervals from the injection onwards and by extracting the w parameter (Figure 8B), it is possible to plot w^2 as a function of t and calculate D from the slope (Figure 8C).

Since R110 has the capacity to disperse rapidly both axially and longitudinally, any focal accumulation of the dye for long time periods can be reliably attributed to its rapid production at the site of accumulation. The meaning of this is that the intensity of fluorescence observed during an experiment is proportional to proteolytic activity, with only a small loss of temporal resolution. Spatial resolution is probably less well defined because the longitudinal diffusion rate is higher than the leak rate. However, fluorescence gradients were readily discernible (e.g., see Figure 2). It is therefore clear that the peak of the observed gradient correlates with the site of the highest proteolytic activity.

Immunocytochemistry

Cultured neurons were fixed by superfusion with 4% paraformaldehyde and 400 mM sucrose in ASW for 15 min (Forscher and Smith, 1988). The dishes were then washed thoroughly with PBS (phosphate buffered saline: NaCl 8 g/l, Na_2HPO_4 1.44 g/l, KCl 0.2 g/l, and KH_2PO_4 0.24 g/l [pH 7.4]) and permeabilized with PBST (0.1% Triton X-100 in PBS). The neurons were then incubated in filtrated blocking solution (PBST + 1% Bovine Serum Albumin + 5% skimmed milk) for 1 hr at room temperature, followed by incubation in the primary antibody solution (polyclonal rabbit anti-human spectrin, Sigma; 1:300 dilution in blocking solution) for 12 hr at 4°C. The dishes were washed thoroughly with PBST and were then incubated in the secondary antibody solution (sheep anti-rabbit IgG, Cy3 conjugated, Sigma; 1:500 dilution in PBST) for 1 hr at room temperature in the dark. The dishes were washed thoroughly with PBST, then washed with PBS, and finally filled with a 2% n-propyl-galate solution in 1:1 glycerol:DDW. Controls for nonspecific binding of secondary antibodies were performed by omitting the incubation with the primary antibody. The neurons in these dishes showed insignificant fluorescence. In order to confirm the cross reactivity of the anti-human spectrin antibody with *Aplysia* spectrin, we performed Western blots on material obtained from *Aplysia* neuronal ganglia. We found that the antibody bound two bands that comigrated with the spectrin bands in lanes containing proteins extracted from human red blood cell ghosts (data not shown).

In order to observe the density of spectrin in a volume-independent manner, the axons were studied with a confocal microscope. The system consisted of a Biorad MRC-1024 confocal head coupled to a Zeiss Axiovert 135M inverted microscope equipped with a Zeiss 40× 1.3 NA Plan-Neofluar oil immersion objective. The preparations were excited with the 514 nm band of a 100 mW air-cooled argon ion laser (Ion Laser Technologies). Depending on the intensity of the signal, 0.3%, 1%, or 3% of the laser power was used. Emission was filtered through a 570 ± 15 nm band-pass filter. In some images, an additional emission channel, filtered with a 655 ± 45 nm band-pass filter, was added. The confocal iris diameter was set to 2–3 mm, which, in combination with the objective, results in optical sectioning of ~1 μm in depth. Images were produced by either a single scan, by the accumulation of two scans, or by the averaging of two scans, depending on the signal strength and quality. The final images were prepared using commercially available software (Adobe Photoshop).

Acknowledgments

This work was supported by grants from the US-Israel Bi-National Research Foundation (number 93–00132/1) and the German-Israeli Foundation for Scientific Research and Development (number I-392–216.01/94). M. E. S. is the Levi Deviali Professor in Neurobiology. D. G. is supported by the Clore Foundation.

Received December 19, 1997; revised March 30, 1998.

References

Ambron, R.T., Zhang, X.P., Gunstream, J.D., Povelones, M., and Walters, E.T. (1996). Intrinsic injury signals enhance growth, survival, and excitability of *Aplysia* neurons. J. Neurosci. *16*, 7469–7477.

Ariyoshi, H., Shiba, E., Sakon, M., Kambayashi, J., Kawasaki, T., Kang, J., Kawashima, S., and Mori, T. (1992). Membrane binding and autolytic activation of calpain-I in human platelets. Biochem. Int. *27*, 335–341.

Ashery, U., Penner, R., and Spira, M.E. (1996). Acceleration of membrane recycling by axotomy of cultured Aplysia neurons. Neuron *16*, 641–651.

Aunis, D., and Bader, M.F. (1988). The cytoskeleton as a barrier to exocytosis in secretory cells. J. Exp. Biol. *139*, 253–266.

Baas, P.W. (1997). Microtubules and axonal growth. Curr. Opin. Cell Biol. *9*, 29–36.

Bailey, C.H., and Kandel, E.R. (1993). Structural changes accompanying memory storage. Annu. Rev. Physiol. *55*, 397–426.

Banno, Y., Nakashima, S., Hachiya, T., and Nozawa, Y. (1995). Endogenous cleavage of phospholipase Cβ 3 by agonist-induced activation of calpain in human platelets. J. Biol. Chem. *270*, 4318–4324.

Bednarski, E., Vanderklish, P., Gall, C., Saido, T.C., Bahr, B.A., and Lynch, G. (1995). Translational suppression of calpain I reduces NMDA-induced spectrin proteolysis and pathophysiology in cultured hippocampal slices. Brain Res. *694*, 147–157.

Benbassat, D., and Spira, M.E. (1993). Survival of isolated axonal segments in culture: morphological, ultrastructural, and physiological analysis. Exp. Neurol. *122*, 295–310.

Benbassat, D., and Spira, M.E. (1994). The survival of transected axonal segments of cultured *Aplysia* neurons is prolonged by contact with intact nerve cells. Eur. J. Neurosci. *6*, 1605–1614.

Bennett, V., and Gilligan, D.M. (1993). The spectrin-based membrane skeleton and micron-scale organization of the plasma membrane. Annu. Rev. Cell Biol. *9*, 27–66.

Bentley, D., and O'Connor, T.P. (1994). Cytoskeletal events in growth cone steering. Curr. Opin. Neurobiol. *4*, 43–48.

Brorson, J.R., Manzolillo, P.A., and Miller, R.J. (1994). Ca^{2+} entry via AMPA/KA receptors and excitotoxicity in cultured cerebellar Purkinje cells. J. Neurosci. *14*, 187–197.

Buchs, P.A., and Muller, D. (1996). Induction of long-term potentiation is associated with major ultrastructural changes of activated synapses. Proc. Natl. Acad. Sci. USA *93*, 8040–8045.

Covault, J., Liu, Q.Y., and el Deeb, S. (1991). Calcium-activated proteolysis of intracellular domains in the cell adhesion molecules NCAM and N-cadherin. Brain Res. Mol. Brain Res. *11*, 11–16.

Craig, A.M., Wyborski, R.J., and Banker, G. (1995). Preferential addition of newly synthesized membrane protein at axonal growth cones. Nature *375*, 592–594.

del Cerro, S., Larson, J., Oliver, M.W., and Lynch, G. (1990). Development of hippocampal long-term potentiation is reduced by recently introduced calpain inhibitors. Brain Res. *530*, 91–95.

del Cerro, S., Arai, A., Kessler, M., Bahr, B.A., Vanderklish, P., Rivera, S., and Lynch, G. (1994). Stimulation of NMDA receptors activates calpain in cultured hippocampal slices. Neurosci. Lett. *167*, 149–152.

Doherty, P., Fazeli, M.S., and Walsh, F.S. (1995). The neural cell adhesion molecule and synaptic plasticity. J. Neurobiol. *26*, 437–446.

Faddis, B.T., Hasbani, M.J., and Goldberg, M.P. (1997). Calpain activation contributes to dendritic remodeling after brief excitotoxic injury in vitro. J. Neurosci. *17*, 951–959.

Fawcett, J.W. (1993). Growth-cone collapse: too much of a good thing? Trends Neurosci. *16*, 165–167.

Fawcett, J.W., and Keynes, R.J. (1990). Peripheral nerve regeneration. Annu. Rev. Neurosci. *13*, 43–60.

Forscher, P., and Smith, S.J. (1988). Actions of cytochalasins on the organization of actin filaments and microtubules in a neuronal growth cone. J. Cell Biol. *107*, 1505–1516.

Futerman, A.H., and Banker, G.A. (1996). The economics of neurite outgrowth—the addition of new membrane to growing axons. Trends Neurosci. *19*, 144–149.

Gabso, M., Neher, E., and Spira, M.E. (1997). Low mobility of the Ca^{2+} buffers in axons of cultured *Aplysia* neurons. Neuron *18*, 473–481.

Goldberg, D.J., and Wu, D.Y. (1996). Tyrosine phosphorylation and protrusive structures of the growth cone. Perspect. Dev. Neurobiol. *4*, 183–192.

Goll, D.E., Thompson, V.F., Taylor, R.G., and Zalewska, T. (1992). Is calpain activity regulated by membranes and autolysis or by calcium and calpastatin? Bioessays *14*, 549–556.

Goodman, S.R., Zimmer, W.E., Clark, M.B., Zagon, I.S., Barker, J.E., and Bloom, M.L. (1995). Brain spectrin: of mice and men. Brain Res. Bull. *36*, 593–606.

Hall, Z.W., and Sanes, J.R. (1993). Synaptic structure and development: the neuromuscular junction. Cell *72*/Neuron *10* (suppl.), 99–121.

Haydon, P.G., and Drapeau, P. (1995). From contact to connection: early events during synaptogenesis. Trends Neurosci. *18*, 196–201.

Haydon, P.G., and Zoran, M.J. (1994). Retrograde regulation of presynaptic development during synaptogenesis. J. Neurobiol. *25*, 694–706.

Johnson, G.V., Litersky, J.M., and Jope, R.S. (1991). Degradation of microtubule-associated protein 2 and brain spectrin by calpain: a comparative study. J. Neurochem. *56*, 1630–1638.

Kawasaki, H., and Kawashima, S. (1996). Regulation of the calpain-calpastatin system by membranes. Mol. Membr. Biol. *13*, 217–224.

Kumamoto, T., Kleese, W.C., Cong, J.Y., Goll, D.E., Pierce, P.R., and Allen, R.E. (1992). Localization of the Ca^{2+}-dependent proteinases and their inhibitor in normal, fasted, and denervated rat skeletal muscle. Anat. Rec. *232*, 60–77.

Letourneau, P.C., Kater, S.B., and Macagno, E.R. (1992). The Nerve Growth Cone (New York: Raven Press).

Leytus, S.P., Patterson, W.L., and Mangel, W.F. (1983). New class of sensitive and selective fluorogenic substrates for serine proteinases. Amino acid and dipeptide derivatives of rhodamine. Biochem. J. *215*, 253–260.

Lin, C.H., Thompson, C.A., and Forscher, P. (1994). Cytoskeletal reorganization underlying growth cone motility. Curr. Opin. Neurobiol. *4*, 640–647.

Llinas, R., Sugimori, M., and Silver, R.B. (1992). Microdomains of high calcium concentration in a presynaptic terminal. Science *256*, 677–679.

Lynch, G., and Baudry, M. (1984). The biochemistry of memory: a new and specific hypothesis. Science *224*, 1057–1063.

Lynch, G., Kessler, M., Arai, A., and Larson, J. (1990). The nature and causes of hippocampal long-term potentiation. Prog. Brain Res. *83*, 233–250.

Maccioni, R.B., and Cambiazo, V. (1995). Role of microtubule-associated proteins in the control of microtubule assembly. Physiol. Rev. *75*, 835–864.

Maness, P.F. (1992). Nonreceptor protein tyrosine kinases associated with neuronal development. Dev. Neurosci. *14*, 257–270.

Martenson, C., Stone, K., Reedy, M., and Sheetz, M. (1993). Fast axonal transport is required for growth cone advance. Nature *366*, 66–69.

Melloni, E., Michetti, M., Salamino, F., Minafra, R., and Pontremoli, S. (1996). Modulation of the calpain autoproteolysis by calpastatin and phospholipids. Biochem. Biophys. Res. Commun. *229*, 193–197.

Nishimura, T., and Goll, D.E. (1991). Binding of calpain fragments to calpastatin. J. Biol. Chem. *266*, 11842–11850.

Perrin, D., Moller, K., Hanke, K., and Soling, H.D. (1992). cAMP and Ca^{2+}-mediated secretion in parotid acinar cells is associated with reversible changes in the organization of the cytoskeleton. J. Cell Biol. *116*, 127–134.

Pfenninger, K.H., and Friedman, L.B. (1993). Sites of plasmalemmal expansion in growth cones. Brain Res. Dev. Brain Res. *71*, 181–192.

Raser, K.J., Posner, A., and Wang, K.K. (1995). Casein zymography: a method to study μ-calpain, m-calpain, and their inhibitory agents. Arch. Biochem. Biophys. *319*, 211–216.

Rehder, V., Williams, C.V., and Kater, S.B. (1996). Functional compartmentalization of the neuronal growth cone: determining calcium's place in signaling cascades. Perspect. Dev. Neurobiol. *4*, 215–226.

Rothman, S.M., and Olney, J.W. (1995). Excitotoxicity and the NMDA receptor—still lethal after eight years. Trends Neurosci. *18*, 57–58.

Saido, T.C., Sorimachi, H., and Suzuki, K. (1994). Calpain: new perspectives in molecular diversity and physiological-pathological involvement. FASEB J. *8*, 814–822.

Sato, K., Saito, Y., and Kawashima, S. (1995). Identification and characterization of membrane-bound calpains in clathrin-coated vesicles from bovine brain. Eur. J. Biochem. *230*, 25–31.

Schacher, S., and Proshansky, E. (1983). Neurite regeneration by *Aplysia* neurons in dissociated cell culture: modulation by *Aplysia* hemolymph and the presence of the initial axonal segment. J. Neurosci. *3*, 2403–2413.

Seubert, P., Larson, J., Oliver, M., Jung, M.W., Baudry, M., and Lynch, G. (1988). Stimulation of NMDA receptors induces proteolysis of spectrin in hippocampus. Brain Res. *460*, 189–194.

Siman, R., Baudry, M., and Lynch, G. (1984). Brain fodrin: substrate for calpain I, an endogenous calcium-activated protease. Proc. Natl. Acad. Sci. USA *81*, 3572–3576.

Spira, M.E., Benbassat, D., and Dormann, A. (1993). Resealing of the proximal and distal cut ends of transected axons: electrophysiological and ultrastructural analysis. J. Neurobiol. *24*, 300–316.

Spira, M.E., Dormann, A., Ashery, U., Gabso, M., Gitler, D., Benbassat, D., Oren, R., and Ziv, N.E. (1996). Use of *Aplysia* neurons for the study of cellular alterations and the resealing of transected axons in vitro. J. Neurosci. Methods *69*, 91–102.

Spira, M.E., Gitler, D., Oren, R., and Ziv, N.E. (1998). The role of calcium in triggering growth cone formation and neuritogenesis after axotomy of cultured *Aplysia* neurons. In The Neuron in Tissue Culture, L. Haynes, ed. (New York: John Wiley and Sons), in press.

Steffensen, I., Dulin, M.F., Walters, E.T., and Morris, C.E. (1995). Peripheral regeneration and central sprouting of sensory neurone axons in *Aplysia californica* following nerve injury. J. Exp. Biol. *198*, 2067–2078.

Tessier-Lavigne, M., and Goodman, C.S. (1996). The molecular biology of axon guidance. Science *274*, 1123–1133.

Tsujinaka, T., Kajiwara, Y., Kambayashi, J., Sakon, M., Higuchi, N., Tanaka, T., and Mori, T. (1988). Synthesis of a new cell-penetrating calpain inhibitor (calpeptin). Biochem. Biophys. Res. Commun. *153*, 1201–1208.

Vanderklish, P., Saido, T.C., Gall, C., Arai, A., and Lynch, G. (1995).

Proteolysis of spectrin by calpain accompanies theta-burst stimulation in cultured hippocampal slices. Brain Res. Mol. Brain Res. *32*, 25–35.

Wang, K.K., and Yuen, P.W. (1994). Calpain inhibition: an overview of its therapeutic potential. Trends Pharmacol. Sci. *15*, 412–419.

Wu, F., Friedman, L., and Schacher, S. (1995). Transient versus persistent functional and structural changes associated with facilitation of *Aplysia* sensorimotor synapses are second messenger dependent. J. Neurosci. *15*, 7517–7527.

Yu, W., Ahmad, F.J., and Baas, P.W. (1994). Microtubule fragmentation and partitioning in the axon during collateral branch formation. J. Neurosci. *14*, 5872–5884.

Ziv, N.E., and Spira, M.E. (1993). Spatiotemporal distribution of Ca^{2+} following axotomy and throughout the recovery process of cultured *Aplysia* neurons. Eur. J. Neurosci. *5*, 657–668.

Ziv, N.E., and Spira, M.E. (1995). Axotomy induces a transient and localized elevation of the free intracellular calcium concentration to the millimolar range. J. Neurophysiol. *74*, 2625–2637.

Ziv, N.E., and Spira, M.E. (1997). Localized and transient elevations of intracellular Ca^{2+} induce the dedifferentiation of axonal segments into growth cones. J. Neurosci. *17*, 3568–3579.

Ziv, N.E., and Spira, M.E. (1998). Induction of growth cone formation by transient and localized increases of intracellular proteolytic activity. J. Cell Biol. *140*, 223–232.